

Comparison of Two Methods of Interpretation of Langmuir Probe Data for an Inductively Coupled Oxygen Plasma

T. H. Chung^{*1}, Y. M. Shin¹, and D. C. Seo²

¹ Department of Physics, Dong-A University, Busan 604-714, Korea

² Korea Basic Science Institute, Daejeon, 305-333, Korea

Received 23 May 2005, accepted 30 August 2005

Published online 9 June 2006

Key words Langmuir probe, negative ions, oxygen RF plasma.

PACS 52.20ch, 52.25-b, 52.80Pi

The Langmuir probe technique has some drawback in applying to electronegative plasma since it is difficult to interpret the probe $I - V$ data. The positive ion flux to the probe is modified due to the presence of negative ions. In this study, an inductively coupled oxygen RF plasma is employed to perform the Langmuir probe measurement of the electronegative discharge. Plasma parameters are obtained from Langmuir probe measurement using two different methods which are based on electron energy distribution function (EEDF) integrals, and the method based on the fluid model for the modified ion flux, respectively. The EEDF is measured by a double differentiation of the $I - V$ characteristics according to the Druyvesteyn formula. The electron densities estimated based on the two methods are compared. The EEDF integral method gives little higher values than the modified ion flux method. It is observed that at low pressure the EEDF is close to a Maxwellian. Generally, as the pressure increases, the distributions switch to bi-Maxwellian and to Druyvesteyn, and suggest some depletion of electrons with larger energies.

© 2006 WILEY-VCH Verlag GmbH & Co. KGaA, Weinheim

1 Introduction

Negative ions are found in electronegative gases such as oxygen, chlorine, SF_6 , and fluorocarbons which are used extensively in discharges for various applications of plasma processing. The presence of negative ions complicates the discharge phenomena. Negative-ion sources can be applied to charging-free ion implantation in semiconductor manufacture, and negative-ion assisted etching is found to reduce the charging of substrates [1]. There is considerable scientific and technological interest in electronegative plasmas [2, 3] and so in the determination of negative ion density [4–6]. Langmuir probes [7], photodetachment [4, 5], and laser Thomson scattering [8] are diagnostic tools for investigating negative ions in plasma. Among these, Langmuir probe technique is simple, inexpensive and provides the spatial resolution of plasma parameters. There has been an increased demand to determine the plasma parameters (charged particle densities, sheath width, electron temperature, and plasma potential) for electronegative plasmas. The operating regions of electronegative discharges were classified in the entire control parameter space [9]. The discharge properties such as the ratio of the negative ion density to the electron density, the spatial profile of charged species, and the prevailing particle loss mechanism (volume recombination loss or ion flux loss to the wall due to diffusion) also depend on the operating region. In a previous paper [10], we explored the scaling relations for a low power region, and observed that the experimentally measured scalings of the charged species are in agreement with the predictions of the spatially averaged global model [2]. We observed the scaling laws to hold in a medium power region [11, 12]. However, in those studies, we estimated the positive ion density directly from the positive ion saturation current assuming that the positive ions have the normal Bohm velocity. In this paper, we reexamine the plasma parameters such as the densities of charged species, electron temperature, and electron energy distribution function over the range of pressure and power that is typical of those used currently in the industry. Plasma parameters are obtained from the standard

* Corresponding author: e-mail: thchung@dau.ac.kr

Langmuir probe method. However, the determination of the electron density is performed in a little different way than usual method applicable to the electropositive case. Although the Langmuir probe technique provides in nature very rough estimation and the analysis of the probe data is difficult, the probe method is used widely in the processing plasmas because of easy handling and low expense. The main issue lies in the modeling of the positive ion flux to the probe for electronegative plasmas. The interpretation of $I - V$ characteristics of the Langmuir probe will be performed by two different methods. The first one is a method based on electron energy distribution function (EEDF) integrals. The second one is based on the fluid model for the modified ion flux since the probe ion current is modified due to the presence of negative ions. The ion saturation zone of the $I - V$ characteristics of the probe is increasingly used in plasma diagnosis. The current drained by the probe in this zone is very small and reduces the perturbation that the measurement causes in the plasma. To implement a proper probe theory, one has to solve Poisson's equation for the electric potential everywhere from the probe surface to $r = \infty$. This method using the modified ion flux also assumes that electrons and negative ions follow the Boltzmann energy distribution. This model allow us to obtain the profiles of electric potential, positive ion flux, positive ion density in the sheath, and $I - V$ characteristic curve of the probe. The estimated density values of electrons by these two different methods are compared with each other. In this study, an inductively coupled oxygen RF plasma is employed as an example of electronegative discharge since oxygen plasmas have found numerous applications in plasma processing such as plasma enhanced chemical vapor deposition, reactive sputtering, dry etching of polymer, oxidation, and resist removal of semiconductor. For simplicity, we consider that electronegative plasma consists of three charged species, which are positive ion, negative ion and electron.

2 Two Methods to interpret Langmuir probe Data for electronegative plasmas

2.1 EEDF integral method

The second derivative of the measured probe current, I'' , is related to the electron energy distribution function (EEDF), $f(\epsilon)$, as follow:

$$f(\epsilon) = \frac{2m}{e^2 S} \left(\frac{2eV}{m} \right)^{1/2} I'', \quad (1)$$

where e is the electron charge, S is the probe area, m is mass of electrons, V is the probe potential referenced to the plasma potential (space potential), and ϵ is measured in units of eV. The electron density and the effective electron temperature are calculated with the measured EEDF as follows:

$$n_e = \int_0^{\epsilon_{max}} f(\epsilon) d\epsilon, \quad T_{eff} = \frac{2}{3n_e} \int_0^{\epsilon_{max}} \epsilon f(\epsilon) d\epsilon, \quad (2)$$

where ϵ_{max} is determined by the dynamic range of the EEDF measurement. The electron temperature can also be determined from the slope of the probe $\ln(I) - V$ curve in the exponential region (from the point where the probe current is zero to where the slope of the curve begins to decrease). We observe that the both methods yield almost same values of the electron temperature. The EEDF integral method has been used to obtain plasma parameters for many processing plasmas utilizing molecular gases [13, 14].

The probe current I consists of the electron current and the negative ion current. If both species are Maxwellian, the currents of each in the exponential region are written as

$$I_e(V_p) = eS n_e \left(\frac{T_e}{2\pi m} \right)^{1/2} e^{-e(V_s - V_p)/T_e}, \quad I_-(V_p) = eS n_- \left(\frac{T_-}{2\pi M_-} \right)^{1/2} e^{-e(V_s - V_p)/T_e} \quad (3)$$

where n_e and n_- are the electron density and the negative ion density, T_e and T_- are the temperature of the electrons and negative ions, V_s and V_p are the space potential and the probe voltage, M_- is the mass of the negative ion. Differentiating equation (3) n times, we have [15]

$$\frac{I_-^{(n)}}{I_e^{(n)}} = \alpha \gamma^{n-1/2} \left(\frac{m}{M_-} \right)^{1/2} \quad (4)$$

where $\alpha = n_-/n_e$ and $\gamma = T_e/T_-$. Since under the circumstances considered in this study, we have $5 < \gamma < 50$, and $0.05 < \alpha < 1$ (weakly electronegative), the negative ion peak I_-'' is expected to be on the electron peak I_e'' a little below V_s . But, the magnitude of I_-'' is small compared to I_e'' . I_-'' becomes comparable to I_e'' as a higher derivative is taken. Thus, equation (1) can give the electron energy distribution function.

2.2 Modified Bohm Flux Method

The presence of the negative ions complicate the characteristics of the probe $I - V$ curve. The negative ions contribute to the probe current in the exponential region, and the amount of the contribution gets larger when the probe voltage approaches to the plasma potential. The ion saturation zone of the $I - V$ characteristics of the probe is increasingly used in plasma diagnosis [16]. The current drained by the probe in this zone is very small and reduces the perturbation that the measurement causes in the plasma. The sheath structure and the motion of positive ions within the presheath are modified when negative ions are present. The precise values of positive ion density and ion velocity at the sheath edge should be formulated. The positive ion current to the probe is written as

$$I_+ = eS\Gamma_s(\alpha, \gamma, n_e), \quad (5)$$

where $\Gamma_s(\alpha, \gamma, n_e) = n_{+s}v_{+s}$ is the modified Bohm flux, n_{+s} and v_{+s} are the density and velocity of positive ions at sheath edge when negative ions are present [17, 18]. In the numerical calculation of the positive ion flux, the positive ions are modeled as a cold, collisionless fluid, while both the electron and negative ion densities obey Boltzmann relations. The positive ion flux is calculated along the distance from the plasma bulk region to any arbitrarily small distance near the probe edge using a set of coupled equations including the steady state fluid equations of continuity and motion for the positive ion, Poisson equation with Boltzmann electron and Boltzmann negative ion [3, 18]. The equations are one-dimensional assuming no orbital motion of the ion. The ions are all drawn radially into the probe. This theoretical model of the positive ion flux for cylindrical and spherical probes has been developed [19]. Especially, in this model, the $I - V$ characteristic curves of the cylindrical Langmuir probe can be obtained and compared with the experimental curve, which can give the estimation of α , γ and the electron density. The theoretical $I - V$ curve can be drawn in terms of the normalized parameters (η and I);

$$x = \frac{r}{\lambda_D}, \quad a = \frac{j_D}{en_{+0}c_s}, \quad \eta = -\frac{eV}{T_e}, \quad j_D = \frac{I_+}{2\pi\lambda_D}, \quad I = ax_p \quad (6)$$

where λ_D is the Debye length, $I_+ = 2\pi e r n_+ v_+$ is the positive ion current to the cylindrical probe per unit length, n_{+0} is the positive ion density in the bulk, c_s is the Bohm velocity, and r_p is the radius of the probe. The parameter a depends on x_p which in turn depends on the electron density to be determined. For each assumed value of I (normalized probe current), the set of equations including Poisson's equation can be integrated from $x = \infty$ to any arbitrarily small x . The point on the curve where $x = x_p$ gives the normalized potential η_p for that value of I . By computing a family of curves for different I , one can obtain $I - \eta_p$ curve for a probe of radius x_p . For a selected values of I and η_p on the measured probe characteristics we have to estimate x_p . The electron temperature is supposed to be determined from measuring the slope of the probe $I - V$ curve. Then it is possible to determine the electron density, α , and γ . Using a density balance between negatively and positively charged particles given by $n_e + n_- = n_+$, we can estimate the positive ion density [15].

3 Experiment

The plasma generation chamber consists of a stainless steel cylinder with a diameter 28 cm and a length of 30 cm. A 1.9 cm thick by 27 cm diameter tempered glass plate mounted on the one end separates the planar one-turn induction coil from the plasma. A schematic of the planar inductive plasma source and Langmuir probe diagnostics system is shown in the previous paper [20]. A cylindrical Langmuir probe made of tungsten with diameter 1 mm and length 3 mm is used to measure the plasma parameters. The plasma chamber is evacuated by a turbomolecular pump (TPU 520) backed by rotary pump (DUO 30A) giving a base pressure of 9×10^{-7} Torr.

The equilibrium gas pressure in the chamber is monitored with a combination vacuum gauge (IMG 300). The operating gas pressure is controlled by adjusting the mass flow controller. The flow rate of the oxygen gas has the range of 1 - 60 sccm. The oxygen gas pressure is varied in the range of 1 - 40 mTorr. The induction coil is made of copper (with water cooling) and connected to a L-type capacitive matching network and a RF amplifier (KALMUS 137C). The Langmuir probe is powered by a bipolar operational power supply amplifier (BOP 200-1M). A triangle ramp wave, swept from -50 to +50 V at 300 Hz is fed into the bipolar operational power amplifier from a ramp generator (HP33120A). The current measurement is done across a 200 Ω resistor placed between the common and ground outputs of the BOP amplifier. The current and voltage signals are collected on a TK420 digitizing oscilloscope. Experiments were conducted at several pressures and powers. In order to allow the chamber to reach an equilibrium, the plasma was turned on and allowed to run for an hour before taking any measurements. The obtained probe $I - V$ data are analyzed by two different methods stated above.

4 Results and Discussion

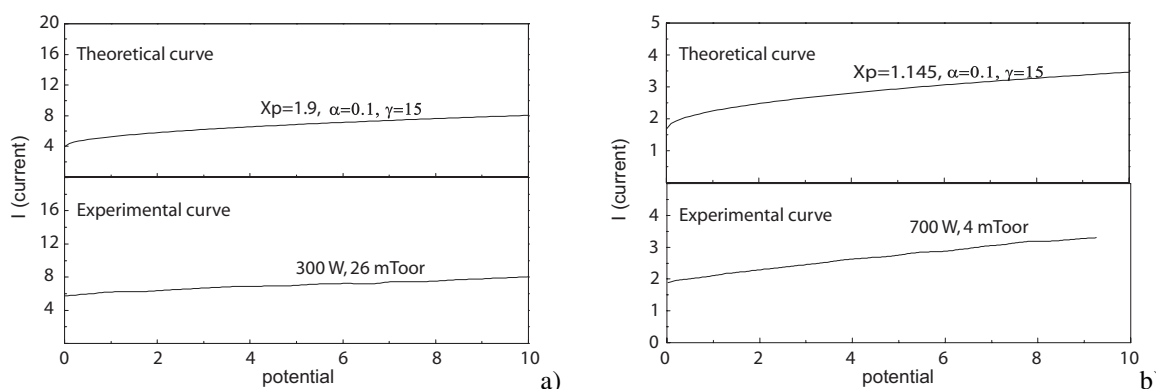


Fig. 1 a) Comparison of the experimental $I - V$ curve of the probe for $P_{abs} = 300$ W, $p = 26$ mtorr with a theoretical $I - V$ curve. b) Comparison of the experimental $I - V$ curve of the probe for $P_{abs} = 700$ W, $p = 4$ mtorr with a theoretical $I - V$ curve.

Figure 1a) shows the comparison of the experimental $I - V$ curve of the probe for $P_{abs} = 700$ W, $p = 4$ mTorr with the theoretical $I - V$ curve. In the case shown here, x_p is 1.145, the values of α and γ are found to be about 0.1 and 15, respectively. As was anticipated, the oxygen discharge is weakly electronegative. Stamate et al. estimated the negative ion temperature by using a test function method for a multipolar magnetically confined oxygen plasma with pressure of 0.5 - 10 mTorr [21]. The ratio was in the range of 10 - 50, and its dependence on the pressure and the discharge current was not significant. In the analysis of the probe data, we obtained the ratio γ of 15. However, the negative ion temperature needs to be known accurately from other methods [22]. To determine the temperature ratio γ more accurately, one has to use a separate double probe along with the single probe [23] or a more sophisticated Thomson scattering technique [8].

Figure 1b) shows the comparison of the experimental $I - V$ curve of the probe for $P_{abs} = 300$ W, $p = 26$ mtorr with the theoretical $I - V$ curve. In this case, x_p is 1.9, the values of α and γ are found to be about 0.1 and 15, respectively. This indicates that the values of α and γ do not vary noticeably in the operating region of this study.

Figure 2 shows the electron densities as a function of pressure which are obtained by two different methods. The EEDF integral method gives little higher values than the modified Bohm flux method. The reason of this discrepancy has not understood yet. One candidate is the negative ion contribution to the probe current peak for the EEDF integral method. The variations of electron density (and positive ion density) with pressure is in agreement with the other experimental results [24-27]. The EEDF integral method seems to lead to a little over-estimation of the electron density (and the negative ion density) because the probe current peak has the negative ion contribution. At low pressures below 10 mTorr, the electron densities obtained by the both methods are almost comparable. We observe that the electron density increases with an increase in pressure at a low pressure range, and has a maximum, and then decreases slightly. This behavior seems to be related to the transition of the dominant loss mechanism of charged particles in electronegative plasmas. At a low pressure range, the dominant

loss of charged particles is due to diffusion, while at medium or high pressure range, the loss takes place mainly via the volume recombination. The increase of the volume recombination makes the charged particle density decrease with increasing pressure since the more charged particle a discharge produces the more recombination it results in. The increase of recombination loss along with the diffusion loss makes the charged particle density decrease [11, 12, 20]. In addition to this effect, the decrease in the ionization rate with increasing pressure through the decrease of the electron temperature can contribute to the transition. A similar variation was observed in a recent experiment with a sophisticated correction of the probe $I - V$ data [22]. The magnitude of the electron density seems to be quite comparable to a capacitively coupled [22] and microwave generated [28] oxygen discharges.

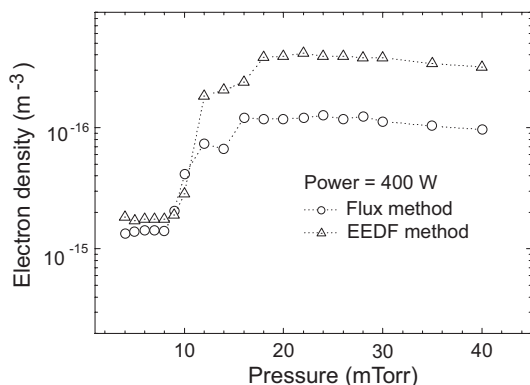


Fig. 2 Electron densities as a function of pressure estimated by two different methods for $P_{abs} = 400$ W

Figure 3 shows the electron energy probability function (EPPF) at several pressures at the input power of 600 W. The EPPFs are in a strict manner non-Maxwellian for the entire energy range. Especially non-Maxwellian EPPFs were observed for all energies above the energy range for elastic collisions [29]. However, in a rough manner, we can state that at low pressure, the EPPF is close to a Maxwellian. The 8 mTorr distributions are somewhat bi-Maxwellian over the region of 2 - 15 eV. The effective electron temperature decreases with increasing pressure.

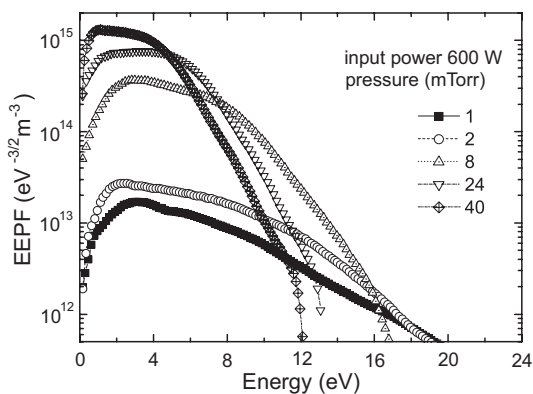


Fig. 3 Electron energy probability functions (EPPFs) as a function of pressure at 600 W input power.

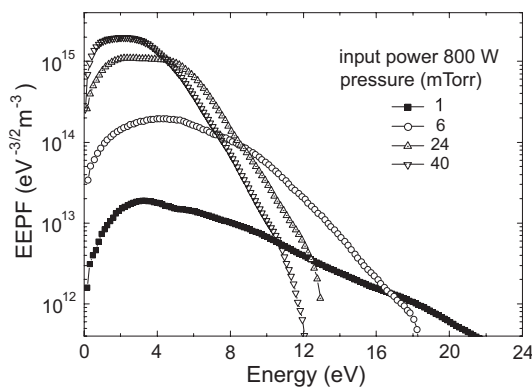


Fig. 4 Electron energy probability functions (EPPFs) as a function of pressure at 800 W input power.

Figure 4 is the EPPFs at the input power of 800 W. The EPPF at 6 mTorr deviates from Maxwellians. The EPPFs above 24 mTorr show much sharper and more pronounced peak at low energies ($\epsilon < 5$ eV), which indicates that the EPPF changes from a single temperature Maxwellian to a Druyvesteyn, and EPPFs are underpopulated compared to a Maxwellian due to excitation and ionization processes as well as escape of high energy electrons from the bulk to the chamber walls [29, 30]. We notice that at low pressure the EEDF is close to a Maxwellian. Generally, as the pressure increases, the distributions switch to bi-Maxwellian and to Druyvesteyn, and suggest some depletion of electrons with larger energies. The input power does not make significant influence on the effective temperature and the shape of EPPF. Further increases in the input power lead to an abrupt change in the EPPF shape with a drop in the effective electron temperature and a rapid increase in plasma density. A primary

application of the electron energy distribution function is the calculation of the rate constants for electron-impact reactions. An extrapolation of the EEDF from elastic energy range into inelastic energy range may cause a significant error in the calculation of excitation and ionization rates in these non-Maxwellian plasmas [29]. The major shortcoming of the standard Langmuir probe method is that Maxwellian electron energy distributions are assumed [28]. The fact that EEDFs are deviated from Maxwellian except at low pressure region (below about 10 mTorr) places limitation on the use of Langmuir probe method for diagnosing plasma parameters.

5 Conclusion

The electronegative inductively coupled oxygen rf discharges have been studied based on Langmuir probe measurements. The electron density is obtained based on two different methods. In charged species densities, the EEDF integral method gives little higher values than the fluid model for the modified positive ion flux, because in EEDF method the probe current in the exponential region includes the contributions both from negative ions and from electrons. The inductively coupled oxygen discharge proves to be weakly electronegative ($\alpha \sim 0.1$), and the values of γ range from 10 to 20 for most of operating region. The EEDFs are in a strict manner non-Maxwellian for the entire energy range. However, in a rough manner, it is observed that at low pressure the EEDF is close to a Maxwellian. Generally, as the pressure increases, the distributions switch to bi-Maxwellian and to Druyvesteyn. The observation that EEDFs are deviated from Maxwellian except at low pressure region (below about 5 mTorr) in an inductively coupled oxygen discharge places some limitation on the use of Langmuir probe method for electronegative plasmas.

Acknowledgements We are grateful to Professors A. J. Lichtenberg and M. A. Lieberman of the University of California at Berkeley for fruitful discussions. This work is supported by Plasma Fusion User Program of Korea Basic Science Institute (the program year of 2005).

References

- [1] S. Samukawa and T. Mieno, *Plasma Sources Sci. Technol.* **5**, 132 (1996).
- [2] C. Lee and M.A. Lieberman, *J. Vac. Sci. Technol. A* **13**, 368 (1995).
- [3] R.N. Franklin, *Plasma Sources Sci. Technol.* **9**, 191 (2000).
- [4] E. Quandt, H.F. Fobele, and W.G. Graham, *Appl. Phys. Lett.* **72**, 2394 (1998).
- [5] D. Hayashi and K. Kadota, *J. Appl. Phys.* **83**, 697 (1998).
- [6] H.J. Yoon, T.H. Chung, and D.C. Seo, *Jpn. J. Appl. Phys.* **38**, 6890 (1999).
- [7] M. Vucelic and S. Mijovic, *J. Appl. Phys.* **84**, 4731 (1998).
- [8] M. Noguchi, T. Hirao, M. Shindo, K. Sakurauchi, Y. Yamagata, K. Uchino, Y. Kawai, and K. Muraoka, *Plasma Sources Sci. Technol.* **12**, 403 (2003).
- [9] A.J. Lichtenberg, M.A. Lieberman, I.G. Kouznetsov, and T.H. Chung, *Plasma Sources Sci. Technol.* **9**, 45 (2000).
- [10] T.H. Chung, H.J. Yoon, and D.C. Seo, *J. Appl. Phys.* **86**, 3536 (1999).
- [11] T.H. Chung, D.C. Seo, G.H. Kim, and J.S. Kim, *IEEE Trans. on Plasma Sci.* **29**, 970 (2001).
- [12] D.C. Seo, T.H. Chung, H.J. Yoon, and G.H. Kim, *J. Appl. Phys.* **89**, 4218 (2001).
- [13] K. Okada, S. Komatsu, and S. Matsumoto, *J. Vac. Sci. Technol. A* **17**(3), 721 (1999).
- [14] J. Hong, A. Granier, C. Leteinturier, M. Peignon, and G. Turban, *J. Vac. Sci. Technol. A* **18**(2), 497 (2000).
- [15] H. Amemiya, *J. Phys. D:Appl. Phys.* **23** 999 (1990).
- [16] R. Morales Crespo, J.I. Fernandez Palop, M.A. Hernandez, and J. Ballesteros, *J. Appl. Phys.* **95**, 2982 (2004).
- [17] P. Chabert, T.E. Sheridan, R.W. Boswell, and J. Perrins, *Plasma Sources Sci. Technol.* **8**, 561 (1999).
- [18] T.E. Sheridan, P. Chabert, and R.W. Boswell, *Plasma Sources Sci. Technol.* **8**, 457 (1999).
- [19] R. Morales Crespo, J.I. Fernandez Palop, M.A. Hernandez, S. Borrego del Pino, and J. Ballesteros, *J. Appl. Phys.* **96**, 4777 (2004).
- [20] D.C. Seo and T.H. Chung, *J. Phys. D:Appl. Phys.* **34**, 2854 (2001).
- [21] E. Stamate, T. Kimura, and K. Ohe, 17th Symp. Plasma Processing (Div. of Plasma Electronics, The Japan Society of Applied Physics) p.259 (2000).
- [22] P. Bryant, A. Dyson and J.E. Allen, *J. Phys. D:Appl. Phys.* **34**, 95 (2001).
- [23] H. Amemiya, *Jpn. J. Appl. Phys.* **27**, 2423 (1988).
- [24] J.H. Keller, J.C. Forster, and M.S. Barns, *J. Vac. Sci. Technol. A* **11**, 2487 (1993).
- [25] M.S. Barns, J.C. Forster, and J.H. Keller, *Appl. Phys. Lett.* **62**, 2622 (1993).
- [26] Y. Ra and C.H. Chen, *J. Vac. Sci. Technol. A* **11**, 2158 (1996).
- [27] E. Stoffels, W.W. Stoffels, D. Vender, M. Kando, G.M.W. Kroesen, and F.J. de Hoog, *Phys. Rev. E* **51**, 2425 (1995).
- [28] J.E. Heidenreich III, J.R. Paraszczak, M. Moisan, and G. Sauve, *J. Vac. Sci. Technol. B* **6**(1), 288 (1988).
- [29] A. Schwabedissen, E.C. Benck, and J.R. Roberts, *Phys. Rev. E* **55**, 3450 (1997).
- [30] H. Singh and D.B. Graves, *J. Appl. Phys.* **87**, 4098 (2000).